

Determination of the pair potential and the ion-electron pseudopotential for aluminum from experimental structure-factor data for liquid aluminum

M. W. C. Dharma-wardana and G. C. Aers

Division of Physics, National Research Council, Ottawa K1A 0R6, Canada

(Received 14 March 1983)

A method of inverting a given structure factor $[S(k)]_{\text{expt}}$ of a liquid metal using a hypernetted-chain equation containing bridge-diagram contributions is presented. Starting from parametrized local pseudopotential and a parametrized model local field (or a theoretical local field), a pair potential is constructed. The $S(k)$ calculated from it is fitted to the given $[S(k)]_{\text{expt}}$. The method is first applied to a molecular-dynamics-generated $S(k)$ derived from an *ab initio* aluminum potential and shown to yield the pair potential, the pseudopotential, and the charge density in excellent *quantitative* agreement with the original *ab initio* potential and other quantities. The method is then applied to the experimental $S(k)$ of aluminum from x-ray data at 943 K. The Al-Al pair potential, Al-electron pseudopotential, and electron charge densities as well as the electron-gas response function (i.e., the model local field) are obtained self-consistently, to within the accuracy of the experimental data. The calculated electrical resistivity is in excellent agreement with experiment. These investigations provide a comparative examination of the electron-gas local fields of Geldart-Taylor, Vashishta-Singwi, Ichimaru-Utsumi, and the density-functional local-density approximation. The hard-sphere parameter defining the bridge term is found to be essentially the same for the different ion-ion potentials determined from all but one of the different local fields, thus supporting the "universality" hypothesis of Rosenfeld and Ashcroft.

I. INTRODUCTION

The determination of interionic potentials from liquid-metal structure-factor data has been a tantalizing possibility since the early efforts of Johnson¹ and co-workers. The object of this paper is to show that ion-ion potentials as well as ion-electron pseudopotentials can be obtained with a high degree of confidence from liquid-structure data.

Several methods²⁻⁷ have been used previously, but with doubtful results. These involved the use of the properties of the direct-correlation function $c(r)$ at large r , direct inversion of the structure factor $S(k)$, or the pair-distribution function $g(r)$ using various equations derived from statistical mechanics of liquids [e.g., Born-Green, Percus-Yevick (PY), hypernetted chain, etc.; for a brief review, see Waseda⁸]. Mitra and collaborators⁹ have examined the use of more general types of equations coupled with fitting to other physical data (e.g., specific heats), together with variation of the potential within molecular-dynamics (MD) simulations. Rao and Joarder¹⁰ have attempted to include compressibility criteria into hypernetted-chain (HNC) inversion of the structure factor. However, none of these methods led to reliable ion-ion potentials of quantitative accuracy. Further, it was not reasonable to hope for information on ion-electron pseudopotentials from the so obtained low-precision ion-ion potentials.

The usual approaches to the inversion of structure data are destined to run into several difficulties from the outset. The experimental $S(k)$ is available only in a limited range of k values, while both the small- and large- k data are necessary for any accurate inversion procedure. Although various methods can be considered for the extension of $S(k)$ data, the inversion results tend to be sensitive to the method used. Also, given an ion-ion potential $U(r)$ and

its own $S(k)$, obtained from molecular dynamics, it is known (e.g., see Taylor and Watts¹¹) that the HNC or PY inversion does *not* reproduce the original potential $U(r)$.

The failure of the HNC and similar equations is a consequence of the approximation inherent in them. The diagrammatic analysis of the pair-distribution function $g(r)$ leads to the form

$$g(r) = \exp[-\beta U(r) + N(r) + B(r)], \quad (1.1)$$

where $\beta = 1/k_B T$ and $N(r)$ and $B(r)$ are the so-called nodal and bridge-diagram contributions. The HNC approximation consists of neglecting the bridge terms.¹² Then the Ornstein-Zernike equation¹² can be coupled with (1.1) to give the following set of closed equations:

$$g(r) = \exp[-\beta U(r) + N(r)], \quad (1.2)$$

$$N(r) = h(r) - c(r), \quad (1.2)$$

$$h(r) = g(r) - 1,$$

$$c(\vec{r}) = h(\vec{r}) - \rho \int h(|\vec{r} - \vec{r}'|) c(\vec{r}') d\vec{r}', \quad (1.3)$$

$$S(k) = 1 + \rho \int h(\vec{r}) e^{i\vec{k} \cdot \vec{r}} d\vec{r}. \quad (1.4)$$

The self-consistent solution of these equations for a given $U(r)$ constitutes the solution of the HNC equation to obtain an $S(k)$. On the other hand, given an $S(k)$, Eqs. (1.2)–(1.4) can be used to determine $U(k)$, thus defining the HNC inversion procedure. Now the solution of the HNC equation from a given $U(r)$ does *not* usually provide a good $S(k)$ or $g(r)$ which agrees with MD simulations. Hence it is not surprising that HNC inversion will not provide a good $U(r)$, unless there is reason to believe that the bridge terms are negligible.

Detailed studies of the HNC solutions of the one-

component plasma¹² (OCP) and other systems have shown that if the bridge term $B(r)$ could be included even in an approximate manner, then a fairly good $g(r)$ could be obtained. An important advance was made by Rosenfeld and Ashcroft¹³ who showed that a good $B(r)$ can be calculated using a hard-sphere potential, irrespective of the actual form of the potential $U(r)$. This “universality” property of $B(r)$ can be exploited if a suitable hard-sphere-packing density parameter η is available for each liquid metal. In fact, as already noted by Ashcroft and Lekner¹⁴ in another context, it turns out that $\eta \approx 0.45$ for most metals near the melting point. This is also in agreement with the range of values of η obtained by Rosenfeld and Ashcroft by fitting to the compressibility sum rule, even in the case of the OCP, for systems near the melting point.

Thus instead of the HNC equation we propose to use the Rosenfeld-Ashcroft form of the modified HNC (MHNC) equation for extracting physical information from experimental $S(k)$. To avoid various ambiguities inherent in the direct inversion of the HNC or MHNC equation, which requires the extension of experimental $S(k)$ data to the full range of k values, we use the MHNC equation in the forward direction. Thus we start from a trial potential $U(k)$ and calculate $S(k)$ using the MHNC equations. The parameters defining $U(k)$ are optimized to fit the experimental $S(k)$ to a given precision. This procedure will still be called an “inversion” of the $S(k)$ data.

The form of the trial ion-ion potential¹⁵ $U(k)$ is taken to be that described by pseudopotential theory. That is, with $\tilde{n}=e=1$,

$$U(k) = Z^2 V_k - \chi(k) V_{ie}(k)^2, \quad (1.5)$$

$$V_k = 4\pi/k^2.$$

Hence the parametrization of $U(k)$ really defines the parametrized electron-ion pseudopotential $V_{ie}(k)$ and the response function $\chi(k)$. Thus the procedure, if successful, determines not only an ion-ion potential, but some effective ion-electron pseudopotential and an associated dielectric function. If the chosen $V_{ie}(k)$ and $\chi(k)$ are *sufficiently flexible*, then the resulting $U(k)$ should be independent of the detailed form of $\chi(k)$ or $V_{ie}(k)$. In other words, $U(k)$ is uniquely determined by the $[S(k)]_{\text{expt}}$ and not by the details of the parametrization. On the other hand, the ion-electron potential $V_{ie}(k)$ will depend on a sensible selection of $\chi(k)$ and a good parametrized form of the pseudopotential.

In this paper we report a detailed examination of the proposed method by an application to aluminum. This is a particularly interesting case¹⁶ as the Al-Al potential is considered to have a repulsive hump at the first-neighbor distance, in some theories of the pair potential, while this feature is absent in others [e.g., see the curve VS (which represents Vashishta-Singwi form) in Fig. 1]. Also only a precise inversion procedure would be able to reproduce reliably such features in the potential.

The Al pair potential $U(r)$ given by Dagens, Rasolt, and Taylor¹⁷ (DRT) and its corresponding molecular-dynamics simulation data¹⁸ were used as a direct test of the inversion procedure. The original DRT potential was recovered with good precision for several forms of $\chi(k)$ using only a two-parameter local pseudopotential, even though DRT used a four-parameter nonlocal form and the

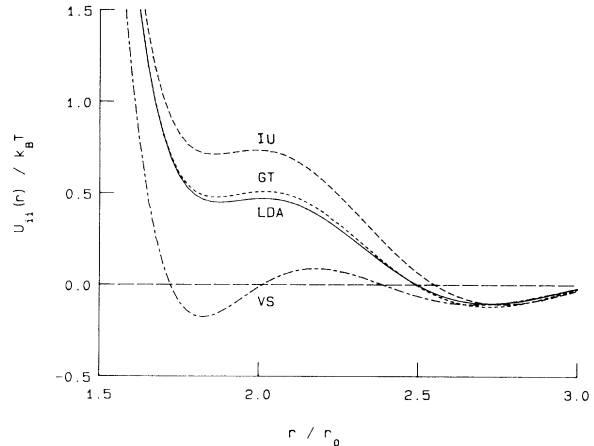


FIG. 1. Pair potentials for Al calculated from the same two-parameter local pseudopotential [see Eq. (2.3)] using different local fields: IU, Ichimaru and Utsumi; GT, Geldart and Taylor; LDA, local-density approximation in density-functional theory; VS, Vashishta and Singwi; for $r_s = 2.168$ a.u. $k_B T = 0.0033245$ a.u.

Geldart-Taylor dielectric function in constructing their $U(r)$. The method was then applied to real aluminum, using the structure-factor data, obtained from x-ray diffraction experiments, given in Waseda.⁸

The plan of this paper is as follows. In Sec. II we present the details of the parametrization of the potential, the hard-sphere parametrization of the bridge-term contribution, and the choice of the electron-gas response function. The electron-charge density induced by an ion, viz., $\chi(k)V_{ie}(k)$, is also discussed in this section as a test of the inversion results. In Sec. III we discuss the details of the inversion of the $S(k)$, generated from MD data for Al, and show that the original DRT potential is correctly recovered. In Sec. IV we discuss the inversion of the experimental structure factor for Al. Here we find that the existing dielectric functions are not flexible enough to achieve an inversion to within the precision of the experimental data. Using a parametrized form for the electron-gas local field, we determine the ion-ion potential, ion-electron pseudopotential, and the local field which are mutually consistent with each other and the experimental structure data. We conclude with a discussion of the results in Sec. V.

II. TRIAL POTENTIAL

We assume that a liquid metal can be described, to a very good approximation, by a pair potential. Pseudopotential theory tells us that this potential should have the form ($e = \tilde{n} = m = 1$)

$$U(k) = Z^2 V_k - \chi(k) V_{ie}(k)^2. \quad (2.1)$$

Hence any suitable parametrization of $V_{ie}(k)$ affords a possible parametrization of $U(k)$, for a given choice of $\chi(k)$. We consider them separately.

A. Ion-electron pseudopotential

The pseudopotential $V_{ie}(k)$ is not uniquely defined, and contains nonlocal and energy-dependent contributions.

However, we seek from pseudopotential theory a convenient, physically meaningful parametrization. If we consider a simple s -wave potential with a well depth A_0 and radius R_0 such that

$$V_{ie}(r) = \begin{cases} A_0, & r < R_0 \\ Z/r, & r \geq R_0, \end{cases} \quad (2.2)$$

we have the k -space form

$$V_{ie}(k) = -ZV_k \left[\frac{A_0 R_0}{Z} j_0(kR_0) - kR_0 \left(\frac{A_0 R_0}{Z} + 1 \right) n_0(kR_0) \right], \quad (2.3)$$

where $j_0(x)$ and $n_0(x)$ are the spherical Bessel and Neumann functions. It is well known that (2.3) is inadequate for most metals. A detailed study of several liquid metals, using a more general parametrization inclusive of nonlocal contributions, etc., will be reported in due course. As we found from detailed trials including up to six parameters that two parameters are quite adequate for inverting the aluminum data, the two-parameter local form (2.2) and (2.3) will be adopted as the standard form of the trial pseudopotential considered in this paper.

B. Electron-gas response function

This is related to the dielectric function $\bar{\epsilon}(k)$ by

$$[\bar{\epsilon}(k)]^{-1} = 1 + V_k \chi(k) \quad (2.4)$$

and can be expressed in terms of a zeroth-order response function $\chi^0(k)$ and a local field $G(k)$. That is,

$$\chi(k) = \frac{\chi^0(k)}{1 - V_k [1 - G(k)] \chi^0(k)}. \quad (2.5)$$

Thus the choice of $\chi^0(k)$ and $G(k)$ completely specifies the response function. When $G(k)=0$ Eq. (2.5) gives the random-phase approximation (RPA) response function. Introducing the electron-sphere radius r_s and an effective electron-sphere radius r_s^* , we can write (2.5) in dimensionless units as follows:

$$V_k \chi(k) = \frac{4\lambda^* F^0(\tilde{k})}{\tilde{k}^2 - [1 - G(\tilde{k}, \lambda^*)] 4\lambda^* F^0(\tilde{k})}, \quad (2.6)$$

where

$$\tilde{k} = k/k_F, \quad k_F = (\alpha r_s^*)^{-1} \text{ a.u.}$$

and

$$\lambda^* = \alpha r_s^* / \pi, \quad \alpha = (4/9\pi)^{1/3}.$$

The effective electron-sphere radius r_s^* has been introduced since it can be used as an adjustable parameter to incorporate electron-renormalization effects.

We have examined the following local fields in this study: (a) the RPA where $G(\tilde{k})=0$, (b) the density-functional local-density approximation (LDA) form,^{19,20} (c) the Geldart-Taylor (GT) form,²¹ (d) the Vashishta-Singwi (VS) form,²² (e) the recently proposed Ichimaru-

Utsumi (IU)²³ form, and (f) a model local field (MLF), having adjustable parameters and capable of generating a good approximation to any of the above forms.

The MLF was invoked only in the analysis of experimental data as the *ab initio* dielectric functions proved to be too inflexible in spite of the use of an r_s^* . In effect the parametrized local field given by MLF affords a procedure for a self-consistent determination of the local field itself from the experimental structure data. Such a possibility exists because, as seen from Fig. 1, the pair potential is very sensitive to the local field. The form chosen for the MLF is

$$G(\tilde{k}) = b_0(1 - e^{-b_1 \tilde{k}^2}) + \frac{b_2 \tilde{k}^2 \exp[-b_3(b_4 - \tilde{k})^2]}{1 + e^{-b_5(b_6 - \tilde{k})}}, \quad (2.7)$$

$$\tilde{k} = k/k_F, \quad b_0 = b_0(\lambda^*), \quad b_1 = b_1(\lambda^*).$$

In actual trials only the most sensitive pairs of parameters, e.g., b_2 and b_4 , were varied. b_0 and b_1 could be fixed by the requirement that $G(\tilde{k})$ for $\tilde{k} \rightarrow 0$ is related to the compressibility and hence to λ^* (i.e., r_s^*) as in Eqs. (2.8)–(2.10). The appropriate b_0 and b_1 were later determined at the end of the calculation. Note that if $b_2=0$, Eq. (2.7) reduces to the VS local field²² when b_0 and b_1 are appropriately chosen. The GT and IU forms can also be approximated by a suitable choice of the parameters. Thus we see that this model local field provides a very flexible parametrization encompassing all the standard local fields as variants of it.

We noted that the $\tilde{k} \rightarrow 0$ limit of $G(\tilde{k})$ has to be chosen so that the compressibility theorem is satisfied. The local field prescribed by the LDA is simply a statement that the \tilde{k} dependence of $G(\tilde{k})$ is far less important than the satisfaction of the compressibility sum rule. The LDA local field is a rigorous result of density-functional theory within the local-density approximation and is given by

$$G(\tilde{k})/\tilde{k}^2 = \phi(0), \quad \text{for all } \tilde{k}, \quad (2.8)$$

$$\phi(0) = 0.25 \left[1 + \lambda(1 - \ln 2) \left[r_s \frac{\partial \bar{E}_c}{\partial r_s} - \frac{r_s}{3} \frac{\partial}{\partial r_s} \frac{\partial \bar{E}_c}{\partial r_s} \right] \right], \quad (2.9)$$

where $\partial \bar{E}_c / \partial r_s$ is the r_s derivative of the electron-gas correlation energy \bar{E}_c . This is obtained from the Vosko-Wilk-Nusair²⁴ parametrization of \bar{E}_c and can be written as

$$r_s \frac{\partial \bar{E}_c}{\partial r_s} = \frac{1 + a_1 x}{1 + a_1 x + a_2 x^2 + a_3 x^3}, \quad x = (r_s)^{1/2}, \quad (2.10)$$

with $a_1 = 9.8137865$, $a_2 = 2.822236$, and $a_3 = 0.736411$.

As already noted by Hedin and Lundqvist,¹⁹ the large- k (i.e., $k > 2k_F$) behavior of the local field is not very important in determining the pair potential $U(r)$ since the free-electron response $F^0(\tilde{k})$ occurring in (2.6) drops off rapidly for large k . As seen from Fig. 2 the GT and LDA local fields are quite similar²⁰ except for $k > 2k_F$, but the pair potentials generated by them are seen from Fig. 1 to be essentially identical.

We have examined two possible choices of the zero-order response $F^0(\tilde{k})$. These are (i) the Lindhard function,

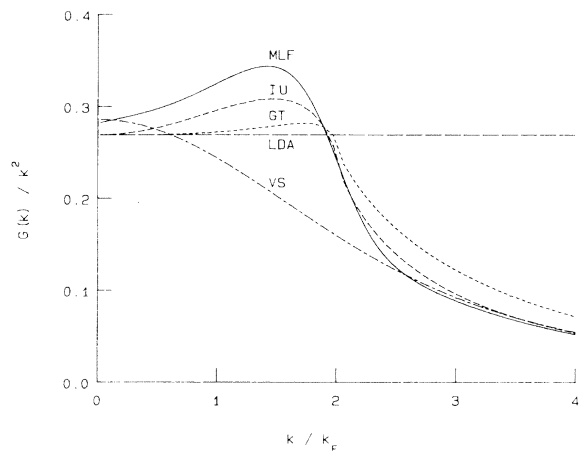


FIG. 2. Local fields VS, LDA, GT, and IU at $r_s = 2.168$ used in forming the potentials of Fig. 1. MLF is a model local field obtained self-consistently from the fit to experiment and is at an effective $r_s^*/r_s = 1.276$.

and (ii) an approximate generalization of the Lindhard form to include electron mean-free-path effects as described by Leavens *et al.*²⁵ However, the simple Lindhard form proved to be quite sufficient while the mean-free-path form did not bring any improvement to the optimization process.

C. Hard-sphere packing density parameter η

An exact evaluation of the bridge term $B(r)$ using the trial potential $U(r)$ is not practical. The Rosenfeld-Ashcroft procedure uses a hard-sphere potential for evaluating $B(r)$, with the hard-sphere parameter η determined to satisfy the compressibility sum rule. This implies that η be adjusted so that the compressibility calculated from the total energy agrees with the value obtained from the $k \rightarrow 0$ limit of $S(k)$. The method requires a knowledge not only of the potential $U(r)$, but also its gradients, its density dependence, etc. Thus a direct utilization of their method is unfortunately not feasible within the present context.

The procedure adopted here was either to fix η to correspond to the best hard-sphere fit to the given $S(k)$, or to treat η as a free parameter where this did not lead to unphysical results. By this we mean if η becomes adjusted to values outside the physically acceptable range (near the melting point it is expected that $0.4 < \eta < 0.48$; the hard-sphere fluid undergoes a phase transition for $\eta \simeq 0.48$), or if the parameter r_s^* in $G(k, r_s^*)$ becomes adjusted to unusually large (or small) values. These unphysical values can arise if the short-range structure introduced by the local field is inadequate in some sense and the bridge terms have to compensate for this in trying to fit $[S(k)]_{\text{calc}}$ to $[S(k)]_{\text{expt}}$. In fact, the question of the suitability of a given local field seems to depend on whether the detailed features of the potential needed to fit the $[S(k)]_{\text{expt}}$ requires the existence of a Thomas-Fermi-type pole (on the imaginary axis) in the dielectric function, for the values of r_s^* generated by the fitting process.

As seen from Fig. 1, VS screening tends to lower the

value of the potential at the first-neighbor position r_1 while IU screening tends to raise the potential, above the value given by the density-functional LDA form. As will be seen later, the behavior of the potential at r_1 is crucial to the value of the compressibility [or, equivalently, the value of $S(0)$], and vice versa. VS screening corresponds to a higher value of $S(0)$ while IU screening favors a lower value of $S(0)$. Hence some of the shortcomings in the screening can be reduced by choosing a fitting procedure where the calculated $S(0)$ is strongly weighted towards the experimental value of $S(0)$, as in Eq. (2.13) to be discussed later.

If the analytic features of $\chi(k)$ are appropriate, then the pair potential $U_{ii}(r)$ would have the right qualitative features. Then the “universality” arguments of Rosenfeld and Ashcroft would suggest that the *hard-sphere parameter* η would be essentially independent of the detailed form of the potential. Thus in our trials (see Sec. III) with the MD data generated from the DRT potential the value of η was ~ 0.425 for all the trial potentials except that generated from the VS local field. In fitting the experimental structure data (Sec. IV) the optimal η was found to be about 0.465, irrespective of the potential, except for that generated from the IU local field, where an $\eta > 0.48$ was needed.

D. Charge densities

The quality of the ion-electron pseudopotential $V_{ie}(k)$ obtained from the inversion process can be tested in a direct manner by a calculation of the charge densities. That is, if $V_{ie}(k)$ had been determined by inverting an $S(k)$ using a particular $\chi(k)$, then the electron-density profile around an isolated ion immersed in jellium, calculated within linear-response theory using $V_{ie}(k)$ and $\chi(k)$, should agree with the full *nonlinear* density obtained from a detailed Schrödinger (or density-functional) calculation. The electron-density profile is thus given by

$$n(k) = -\chi(k)V_{ie}(k) \quad (2.11)$$

and may be calculated once the pseudopotential parameters A_0 , R_0 , and the local field entering into $\chi(k)$ are specified. If the charge density calculated from the pseudopotential was in accord with that from a Schrödinger calculation, it implies that the pseudopotential respects the requirements of charge neutrality, phase shifts, etc., inherent in the full Schrödinger calculation.

E. Computational aspects

The method explored in this paper requires the solution of the MHNC equation for a given set of trial parameters, A_0 , R_0 , r_s^* , η , and a given local field, $G(k, r_s^*)$. The local field may itself have a parametrized form if it is to be determined self-consistently, from the given $[S(k)]_{\text{expt}}$. We found that the MHNC has to be solved to high accuracy (precision greater than 10^{-9}) even in the early stages of the fitting process. Dimensionless grids were used with the r grid in units of the ion-sphere radius $r_0 = r_s Z^{-1/3}$, and the k grid in units of r_0^{-1} . A fast Fourier routine with 4096 points and an r/r_0 space interval of 0.025 were used together with Ng's¹² procedure for separating out the

long-range and short-range potentials and for obtaining convergence. Note that liquid metals near the melting point correspond nominally to an OCP with a strong coupling parameter of the order of 150. The sum of squares of the differences between $[S(k)]_{\text{calc}}$ and $[S(k)]_{\text{expt}}$ were weighted as follows to obtain a function F which was minimized:

$$F = f_0^2 + \sum_{i=N_1}^{N_2} f_i^2, \quad (2.12)$$

$$f_0 = W_0 \{ [S(0)]_{\text{calc}} - [S(0)]_{\text{expt}} \}, \quad (2.13)$$

$$f_i = (1 + \{ [S(0)]_{\text{expt}} - 1 \}^2) \{ [S(k_i)]_{\text{calc}} - [S(k_i)]_{\text{expt}} \}. \quad (2.14)$$

The weighting on $S(0)$ introduced by Eq. (2.13) allows us to constrain the calculated $S(0)$ to a desired value obtained theoretically or from experiments. If $W_0=0$ the calculation “finds its own” value of $S(0)$ defined by the $[S(k)]_{\text{expt}}$ data for the points N_1 to N_2 . However, the value of $S(0)$ crucially determines the form of the pair potential $U(r)$ near the first-neighbor distance r_1 . Thus, for example, $W_0=1000$ was used with VS screening which has a tendency to generate high values of $S(0)$ if no weighting were used. Usually $W_0=100$ was found to be adequate. It should be noted that when $S(0)$ is accurately reproduced f_0 tends to zero and drops out of the minimization.

III. INVERSION OF MD DATA FOR Al

In this section we discuss the inversion of the MD data¹⁸ for Al (at $T=1050$ K and at a density such that the ion-sphere radius $r_0=3.1268$ a.u.) generated from the DRT potential for aluminum. DRT construct their Al-Al potential from the GT dielectric function and the DRT pseudopotential¹⁷ for Al. The latter is a nonlocal pseudopotential containing six parameters (four are independent), $A_0, R_0, A_1, R_1, A_2,$ and R_2 , i.e., up to the $l=2$ angular momentum state, with the constraints $A_0=A_1, R_1=R_2$.

As detailed trials showed that a two-parameter local pseudopotential was sufficient, we use Eq. (2.3) as our trial potential. We also use the response function taken in the form (2.6), which contains the adjustable parameter r_s^* . Thus for a given choice of the local field (e.g., LDA) we have a maximum of four parameters, viz., A_0, R_0, r_s^* , and η , to be adjusted in fitting the $S(k)$ calculated from MHNC to the “experimental data” which is $[S(k)]_{\text{MD}}$ in

the present case.

It should be noted that our procedures have been formulated for fitting $S(k)$ and not the r -space form $g(r)$. This is the appropriate choice since scattering experiments provide $S(k)$ and not $g(r)$. However, MD simulations provide the pair-distribution function $g(r)$ for the limited range $r \leq r_{\text{max}}$, but do not directly provide $[S(k)]_{\text{MD}}$. Hence we used a numerical table of the original DRT potential for Al and generated $[S(k)]_{\text{MD}}$ using MHNC to extend the MD data self-consistently to all values of r , using a value of η adjusted to give a best fit to the available MD data, i.e., $[g(r)]_{\text{MD}}, r \leq r_{\text{max}}$. The optimal value of η , found to be 0.4250, provides a measure of the bridge contributions inherent in the MD data. Note that this type of extension²⁶ of MD data for obtaining $S(k)$ is usually carried out within the less accurate but simpler HNC scheme where $\eta=0$.

The potentials obtained by the inversion of MD data are subject to several sources of error, viz., (a) error inherent in fitting the $[S(k)]_{\text{MHNC}}$ to $[S(k)]_{\text{MD}}$, (b) error arising from the limited r -space MD data, viz., $[g(r)]_{\text{MD}}, r \leq r_{\text{max}}$, (c) numerical noise and the error arising from the limited number of configurations used in the MD simulation (these may be as much as 2%), and (d) noise artificially introduced by restricting the range of $S(k)$ values used in the fitting process to $k_{\text{min}} \leq k \leq k_{\text{max}}$. This was done to simulate the conditions which will arise in fitting $[S(k)]_{\text{expt}}$ since experimental data are available for only a range of k values. Subject to these reservations, the pair potential obtained from the inversion should agree with the original DRT potential if the inversion is successful and if the parametrization, choice of the local field, etc., is flexible enough.

The potentials obtained from the inversion are given in Table I and displayed in Figs. 3(a) and 3(b). From Fig. 3(a) we see that there is excellent agreement with the original DRT potential if the local field in $\chi(k)$ is chosen to be the LDA or the GT form. These are of course the local fields most appropriate to the original DRT potential.¹⁷ In Fig. 3(a) we have also shown the potential GT⁻ which results when a -5% error is enforced on the $S(0)$. This shows the extreme importance of ensuring that $[S(0)]_{\text{calc}}$ is in accord with $[S(0)]_{\text{expt}}$ which has to be determined accurately. The weight factor W_0 , Eq. (2.13), provides a powerful means of enforcing a given $S(0)$ even if the nature of the screening used would normally lead to a qualitatively different potential. Thus although LDA and GT local fields behaved satisfactorily even with $W_0=100$, the IU and VS local fields needed a high weighting

TABLE I. Results of the inversion of MD data at $T=1050$ K for aluminum. The ion-sphere radius $r_0=3.1268$ a.u., $V_0=Ze^2/r_0=0.961230$ a.u. with $Z=3$. Also $[S(0)]_{\text{MD}}$ is 0.02040. The weighted square error $\langle e \rangle^2$ is defined in Eq. (2.12) and W_0 is the weight on the error in $S(0)$. The electron-sphere radius $r_s=2.168$ a.u. The potentials are identified by the local fields used to generate them.

Potential	W_0	η	A_0/V_0	R_0/r_0	r_s^*/r_s	$S(0)/[S(0)]_{\text{MD}}$	$\sum \langle e \rangle^2$
LDA	300	0.428 51	-0.317 75	0.385 06	0.998 04	1.0039	0.014
GT	300	0.424 90	-0.514 81	0.397 38	1.003 88	1.0034	0.009
GT	1000	0.424 34	-0.508 17	0.397 13	1.002 36	1.0001	0.009
IU	1000	0.423 20	-0.972 92	0.431 02	1.048 44	0.9997	0.021
VS	1000	0.401 14	1.243 50	0.327 85	0.897 26	1.0005	0.139

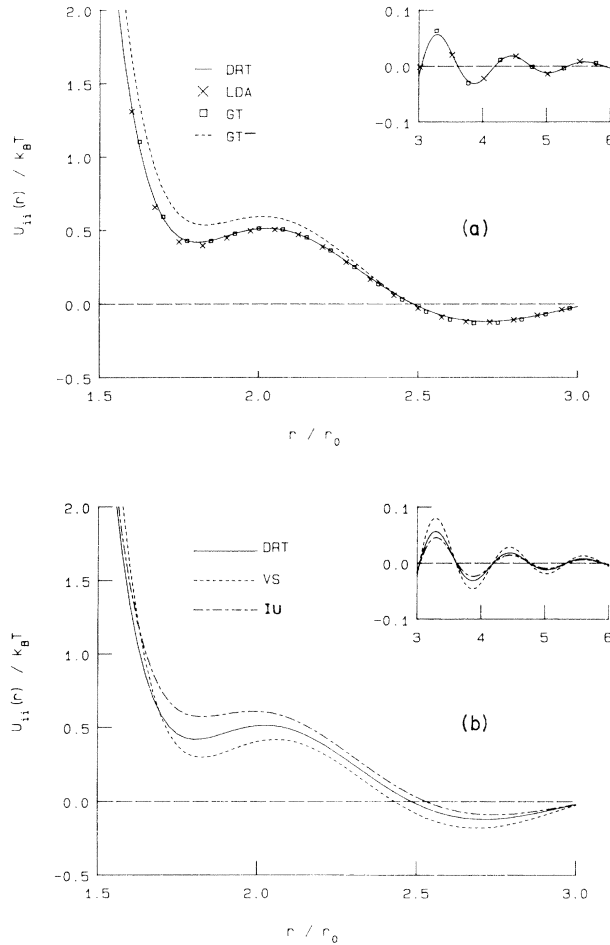


FIG. 3. (a) Pair potentials for Al at 1050 K (see Table I). DRT is the Dagens-Rasolt-Taylor potential used in Ref. 18 for molecular dynamics. LDA and GT are the potentials obtained by inversion of $[S(k)]_{\text{MD}}$ using LDA and GT local fields. GT⁻ is the potential obtained when $[S(0)]_{\text{MD}}$ is assumed to be 5% lower. $k_B T = 0.0033245$ a.u., $r_0 = 3.1268$ a.u. (b) Pair potentials for Al at 1050 K obtained by inversion of $[S(k)]_{\text{MD}}$ using VS and IU local fields (see Table I).

($W_0 = 1000$) to ensure that the given $[S(0)]_{\text{MD}}$ was reproduced with reasonable accuracy; these potentials are shown in Fig. 3(b). If the $S(0)$ weighting W_0 was too low, the VS local field presumably tends to generate short-range correlations which compete with the bridge contributions. The net effect is to drive η towards zero while $[S(0)]_{\text{calc}}$ becomes significantly higher than $[S(0)]_{\text{MD}}$. A similar coupling between η and the local field seems to arise in the IU form which favors low values of $S(0)$. If the density-functional LDA form is taken to be the norm, the VS and IU forms have opposite qualitative features. IU seems to have a strong Thomas-Fermi-type character while the VS form is known²⁷ not to possess a Thomas-Fermi-type pole for $r_s > 1.52$. Thus in order to ensure that the local field used to generate the potential is “appropriate” to a given $S(k)$ it becomes necessary to determine the local field itself via a self-consistent procedure. This objective is realized within the MLF formulation.

The pseudopotentials obtained from the inversion pro-

cess can be tested by calculating the charge-density profile around an isolated Al^{3+} ion immersed in jellium. The results are compared with the self-consistent field (SCF) calculations of Dagens²⁸ in Fig. 4. The Dagens data are for $r_0 = 3.015$, i.e., $r_s = 2.069$, while our pseudopotential parameters are appropriate to $r_0 = 3.1268$. However, the r/r_0 scaling used in the plots make them comparable, to well within the accuracy of these calculations. The agreement confirms that the pseudopotential parameters obtained from the inversion define physically valid pseudopotentials. Note that the charge density for small r obtained from the pseudopotentials do not contain the oscillations found in the SCF density arising from the inner-shell structure of the atom. This is of course entirely in accord with the properties of pseudopotentials.

IV. INVERSION OF EXPERIMENTAL $S(k)$ FOR ALUMINUM

The experimental $S(k)$ obtained from x-ray diffraction data of Waseda^{8,29} were used in this investigation. The data are for $T = 943$ K and at a density corresponding to an ion-sphere radius $r_0 = 3.121$ a.u. Although the experimental $S(k)$ is available for values of k up to about $7k_F$ (6.3 a.u.), only the range $0.3 \leq k < 5k_F$ was used as the data⁸ outside these ranges were judged to be too noisy. The more recent small- k data²⁹ are claimed to have an uncertainty of about 3.4%. Since $S(0)$ is obtained in Ref. 29 by a polynomial fitting process over many data points, one may expect that $S(0)$ itself is obtained to a higher accuracy, e.g., 2%.

The nominal hard-sphere-packing density parameter η for the aluminum-structure data at this temperature is reported⁸ to be 0.45. The first question to be examined was the extent to which an *ab initio* potential (here the DRT potential) constructed for this temperature and density could reproduce $[S(k)]_{\text{expt}}$. The first two lines of Table II are obtained by optimizing η to get the best fit to the experimental $S(k)$ without a weight on $S(0)$, i.e., $W_0 = 0$, and with $S(0)$ weighting. The value of $S(0)$ calculated

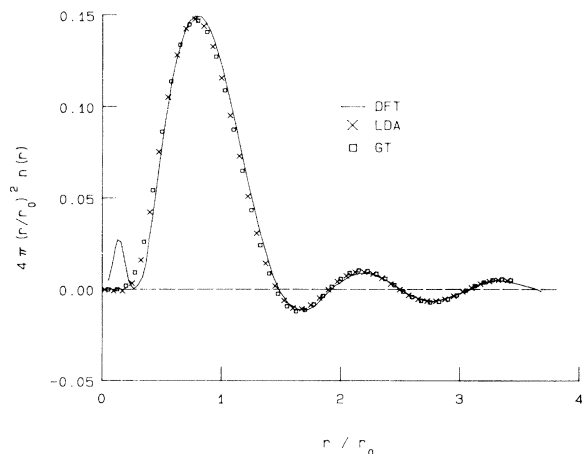


FIG. 4. Electron-charge densities around an isolated Al^{3+} ion in jellium calculated from Eq. (2.11) using the pseudopotentials corresponding to the LDA and GT curves of Fig. 3(a). DFT is the density-functional theory results of Dagens (for $r_s = 2.069$).

TABLE II. Results obtained by fitting to the experimental (Ref. 8) $S(k)$ for Al at $T=943$ K. The ion-sphere radius $r_0=3.121$ a.u., electron sphere radius $r_s=2.164$ a.u. The experimental $S(0)=0.01859$ and W_0 is the weight attached to fitting $S(0)$ as in Eq. (2.13). The weighted square error sums for $W_0=0$ are set in parentheses. $V_0=Ze^2/r_0=0.96123$ a.u.

No.	Potential	W_0	η	A_0/V_0	R_0/r_0	r_s^*/r_s	$S(0)/[S(0)]_{\text{expt}}$	$\sum \langle e \rangle^2$
1	DRT	0	0.46190				0.953	(0.73)
2	DRT	100	0.46152				0.960	0.73
3	RPA	100	0.46540	-1.25554	0.48661	2.31562	1.021	0.52
4	LDA	0	0.46543	-1.22928	0.44873	1.15100	1.171	(0.32)
5		1000	0.46546	-0.99213	0.41477	1.05974	1.004	0.54
6	GT	0	0.46545	-1.29056	0.46131	1.16454	1.156	(0.33)
7		1000	0.46545	-0.98288	0.42255	1.06977	1.003	0.46
8	VS	100	0.46539	0.19656	0.34154	0.98214	1.172	0.63
9		1000	0.46539	1.11769	0.31798	0.92854	1.003	0.78
10	IU	100	0.48847	-1.25459	0.44240	1.13727	0.935	0.28
11		1000	0.48834	-1.47711	0.49059	1.23170	1.001	0.23
12	MLF	100	0.46541	-1.58347	0.63172	1.27875	1.000	0.21

from DRT is about 5% too low; the first peak of $[S(k)]_{\text{expt}}$ is very well reproduced by the DRT potential. The secondary peaks in $S(k)$ (corresponding to the large- k regime) are poorly reproduced by DRT in that the amplitudes are too large.

Illustrative results for the best-fit parameters η , A_0 , R_0 , and r_s^* corresponding to the different choices of response functions are given in Table II. In view of the importance we attach to generating an accurate value of $S(0)$, typical results for different weights W_0 , the ratio $S(0)/[S(0)]_{\text{expt}}$, and the total weighted square error in each case are also given. It is perhaps possible that these results correspond to some local minima and not the absolute minima since an exhaustive search of the four-parameter space is not practical. However, trials from different starting points were used to reduce this possibility. It is gratifying to note that when η is optimized freely, together with A_0 , R_0 , and r_s^* , from different starting points it finds a value of ≈ 0.4654 for almost all the potentials including that derived from the RPA. This feature strongly supports the universality hypothesis of Rosenfeld and Ashcroft. Note that the VS potentials tend to give high values of $S(0)$ unless corrected by a high weighting W_0 . Similarly, IU tends to give low values of $S(0)$. The IU potential tends to generate values of η in excess of 0.5 if the $S(0)$ weighting is removed. (In Fig. 7 the effect of a forced error of $\pm 5\%$ on $S(0)$ on the potential obtained (from the self-consistently determined MLF) is shown, to indicate how errors in $[S(0)]_{\text{expt}}$ are reflected in the potential.)

In Figs. 5(a) and 5(b) the $S(k)$ calculated from the various optimized potentials (except MLF) are shown. The noteworthy features in these figures are that (i) the calculated first peaks are shifted to the left, i.e., to the small- k side of the experimental first peak; (ii) the large- k oscillations of $[S(k)]_{\text{calc}}$ are bigger in amplitude than those of $[S(k)]_{\text{expt}}$, as seen from Fig. 5(b), except in the case of IU which gives a good fit at large k . These optimized potentials are shown in Fig. 6, and are similar to the DRT potential but fall lower since the value of $S(0)$ has been fitted more accurately.

The difficulty in reproducing the $[S(k)]_{\text{expt}}$ to within its error bars with respect to its first peak position, first peak height, and its large- k amplitudes may have an *a priori* explanation in several possibilities.

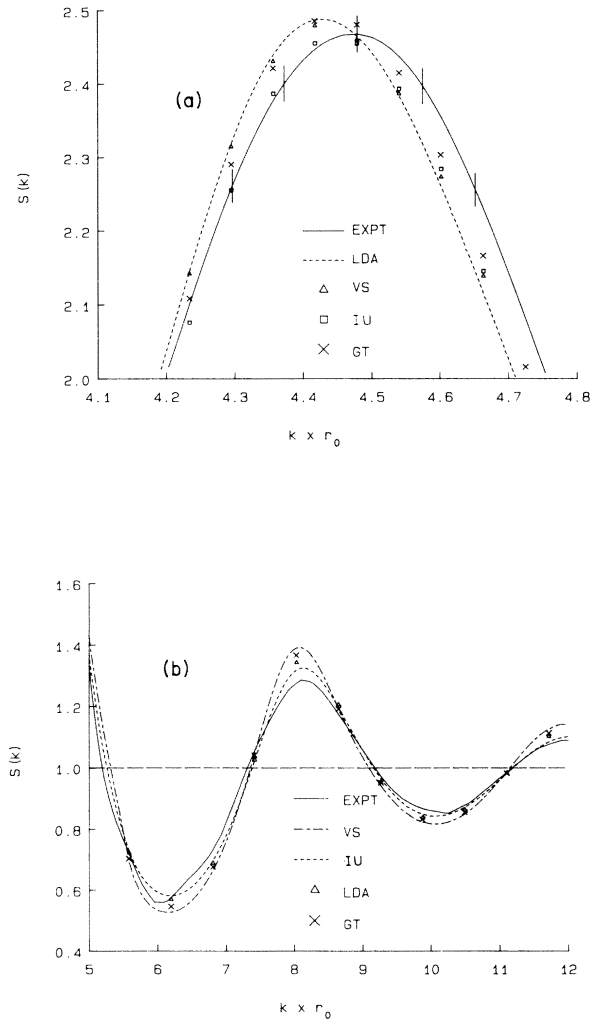


FIG. 5. (a) Comparison of the first peak of $[S(k)]_{\text{expt}}$ and $[S(k)]_{\text{calc}}$ for Al at 943 K. The $[S(k)]_{\text{calc}}$ curves correspond to lines 5, 7, 9, and 11 of Table II. Error bars of $\pm 1\%$ are shown on the experimental curve. (b) Comparison of the large- k region of $[S(k)]_{\text{expt}}$ and $[S(k)]_{\text{calc}}$ for Al at 943 K.

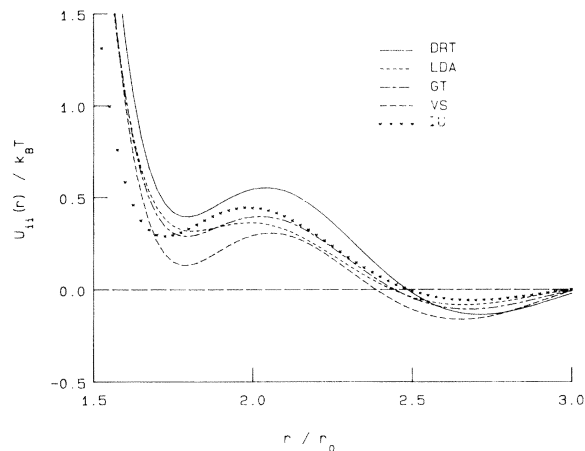


FIG. 6. Pair potentials for Al at 943 K corresponding to lines 5, 7, 9, and 11 of Table II and to $[S(k)]_{\text{calc}}$ of Figs. 5(a) and 5(b). $k_B T = 0.0029862$ a.u. Also shown is the DRT potential at this temperature and density.

(a) Shortcomings in the electron-ion pseudopotential: In Fig. 7(a) we show the $S(k)$ obtained from the DRT potential (which contains nonlocal contributions) with the value of η ($=0.4619$) which gives the best fit to $[S(k)]_{\text{expt}}$. The first peak is well reproduced both in terms of position and height. This clearly suggests that a purely local form of the pseudopotential is not fully satisfactory. From Fig. 7(b) we note, however, that the large- k amplitudes of the $[S(k)]_{\text{DRT}}$ are too large.

(b) Shortcomings in the ion-ion potential: One may expect that the simple ion-ion potential of Eq. (2.3) should be augmented with terms corresponding to Born-Mayer-type terms,³⁰ van der Waals-type³¹ terms, etc. However, no significant improvement in the quality of the fit was obtained when such terms were included.

(c) Inadequacies in the zeroth-order response function: The Lindhard function which was used as the zeroth-order response function $\chi^0(k)$ does not contain any renormalization of the electron propagators arising from the presence of the ion subsystem. An approximate procedure for incorporating this effect is to replace $\chi^0(k)$ by $\chi^0(k, \bar{l})$ where \bar{l} is a mean free path calculated from the self-energy of the electrons in the presence of the ion subsystem. Hence we repeated all the calculations with $\chi^0(k)$ replaced by $\chi^0(k, \bar{l})$ following Ref. 25 but treating \bar{l} as an adjustable parameter. Values of \bar{l} obtained were of the same magnitude as those of Ref. 25 but this procedure led to no useful improvement in the calculated $S(k)$.

(d) Inadequacies in the local field $G(k)$: The actual form of the local field and the effective r_s (i.e., r_s^*) applicable to a liquid metal need not be the same as in jellium at the unrenormalized density corresponding to r_s . Also the form of the potential is clearly very sensitive to the details of the structure of the local field, as seen from Fig. 1. Hence a strong case could be made for studying a *MLF* which is to be determined self-consistently, from the experimental $S(k)$ itself. The form of the MLF was already displayed in Eq. (2.7). This form has the merit of encompassing all the recent electron-gas local fields within its parameter space.

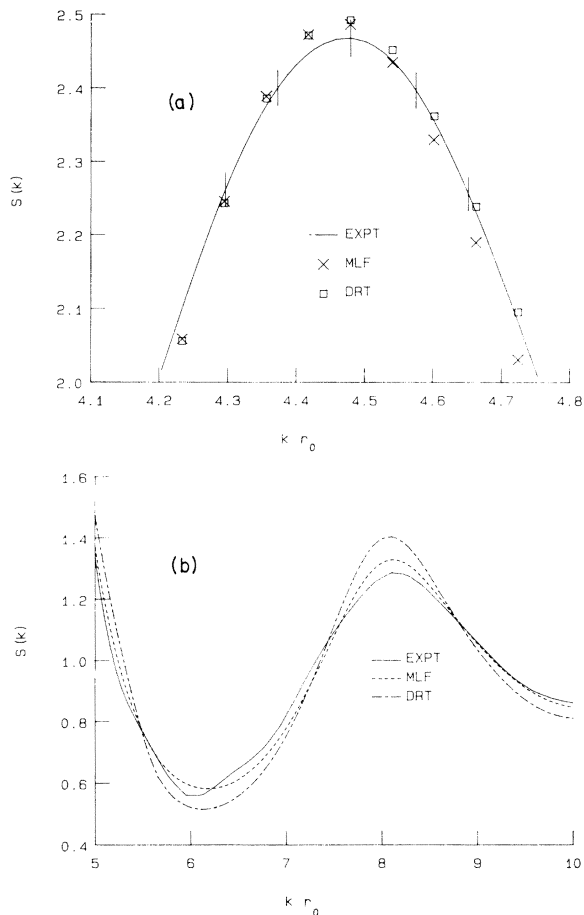


FIG. 7. (a) Comparison of the first peak of $[S(k)]_{\text{expt}}$ and $[S(k)]_{\text{calc}}$ for Al at 943 K, corresponding to lines 2 and 12 of Table II, for DRT and MLF. (b) Comparison of the large- k region of $[S(k)]_{\text{expt}}$ and $[S(k)]_{\text{calc}}$ for Al at 943 K, corresponding to lines 2 and 12 of Table II, for DRT and MLF.

TABLE III. The ion-ion potential derived from the inversion of $[S(k)]_{\text{expt}}$ using the self-consistently generated MLF of line 12, Table II. DRT is the ion-ion potential of Dagens, Rasolt, and Taylor. $r_0 = 3.121$ a.u. (see Sec. IV). The data are in units of $k_B T = 0.0029862$ a.u.

r/r_0	DRT	MLF
1.0	98.500	78.418
1.5	3.5698	2.5624
1.7	0.5447	0.5470
1.9	0.4702	0.4507
2.0	0.5458	0.4492
2.2	0.3625	0.3005
2.4	0.1171	0.0868
2.6	-0.1048	-0.0329
2.8	-0.1202	-0.0398
3.0	-0.0211	0.0002
3.2	0.0559	0.0274
3.4	0.0531	0.0260
3.6	0.0031	0.0113
3.8	-0.0329	0.0012
4.0	-0.0274	0.0010
5.0	-0.0135	0.0006
6.0	-0.0038	0.0005

TABLE IV. Parameters for the MLF defined by Eq. (2.7), obtained by self-consistently fitting to $[S(k)]_{\text{expt}}$, see line 12, Table II. We give for comparison approximate (visually fitted) parametrizations of the GT and IU local fields at $r_s = 2.164$ a.u.

Local field	b_0	b_1	b_2	b_3	b_4	b_5	b_6
MLF	0.8220	0.3381	0.1801	0.850	1.8832	5.3767	2.0097
GT	0.928	0.289	0.15	0.80	2.3	5.0	2.2
IU	0.920	0.289	0.14	0.81	2.0	5.0	2.1

The results obtained from the MLF are shown in Fig. 7 and Table III. The local field itself is displayed, together with the other local fields, in Fig. 2. Calculations with $S(0)$, weighted towards $[S(0)]_{\text{expt}} \pm 5\%$ were also carried out and the corresponding potentials are displayed in Fig. 8. The MLF parameters are given in Table IV. The fully optimized value of η is found to be 0.4654, as with most of the other potentials. The $[S(k)]_{\text{MLF}}$, calculated from the MLF reproduces the experimental data $[S(k)]_{\text{expt}}$ within the error bars of the first peak, except perhaps for its right shoulder, where $[S(k)]_{\text{MLF}}$ falls on the edge of the error bars. An error of about 2% is found to persist in the high- k peaks. The charge density from $[V_{ie}(k)]_{\text{MLF}}$ is displayed in Fig. 9, together with that from $[V_{ie}(k)]_{\text{GT}}$ corresponding to line 7 of Table II, and the SCF results of Dagens for solid jellium aluminum.

V. DISCUSSION AND CONCLUSION

The purpose of the present investigation was to obtain the Al-Al pair potential, pseudopotential, and the local field (or equivalently, the screening function) from the experimental structure data $[S(k)]_{\text{expt}}$. The following features of the results obtained are worthy of comment. (i) If only a fit to the first peak of the $[S(k)]_{\text{expt}}$ is demanded, the *ab initio* potential of DRT seems to be quite satisfactory. The value of $S(0)$ predicted from DRT is within 5% of the experimental value²⁹ (which may be in error of $\pm 2\%$) and hence DRT does reproduce the low- k regime quite well; however, we have noted that small er-

rors in $S(0)$ have large effects on the potential. The two calculations where the optimizations were constrained to $[S(0)]_{\text{expt}} \pm 5\%$ show that the potential is quite sensitive to the quality of the small- k data. (ii) The self-consistently determined MLF and the associated local pseudopotential given in line 12 of Table II give the best overall ion-ion pair potential in the sense of giving the best fit to the experimental data including the small peaks of the large- k region where the DRT gives poor agreement. If the local form of the pseudopotential, Eq. (2.3), used here is replaced by a more general nonlocal form, then we may expect the agreement between the $[S(k)]_{\text{calc}}$ and $[S(0)]_{\text{expt}}$ to improve, especially on the large- k shoulder of the first peak. (iii) The optimized potential $[U(r)]_{\text{MLF}}$ is strongly damped for large r and softer than the DRT potential for small r .

The charge densities shown in Fig. 9 show that the electron distribution is pulled more towards the central ion, compared to the Dagens data for Al^{3+} in jellium at $r_s = 2.069$. This is in agreement with the weaker screening implied by the larger effective r_s , i.e., r_s^* (hence smaller density) entering into MLF in Table II.

The electrical conductivity was calculated using the Ziman formula and gave $23.4 \mu\Omega \text{cm}$, in good agreement with the experimental value of $(24.4 \pm 5\%) \mu\Omega \text{cm}$ (see Ref. 25).

The MLF, determined self-consistently from $S(k)$, is that appropriate for electrons in liquid metallic aluminum. It contains the expected sharp cutoff in the neighborhood of $2k_F$. The $k \rightarrow 0$ limit of $[G(k, r_s^*)]_{\text{MLF}}$, $r_s^* = 2.767$, is

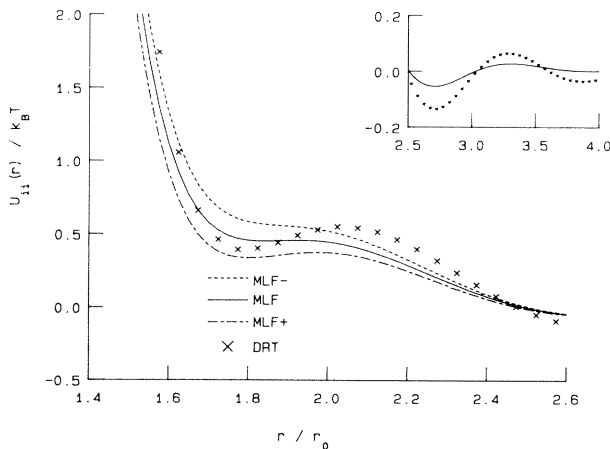


FIG. 8. Solid line is the potential obtained (line 12 of Table II) by inversion of $[S(k)]_{\text{expt}}$ at 943 K using the self-consistently determined MLF (shown in Fig. 2). The potentials corresponding to $[S(0)]_{\text{expt}} \pm 5\%$ are shown as MLF⁺ and MLF⁻. Also shown is the DRT potential.

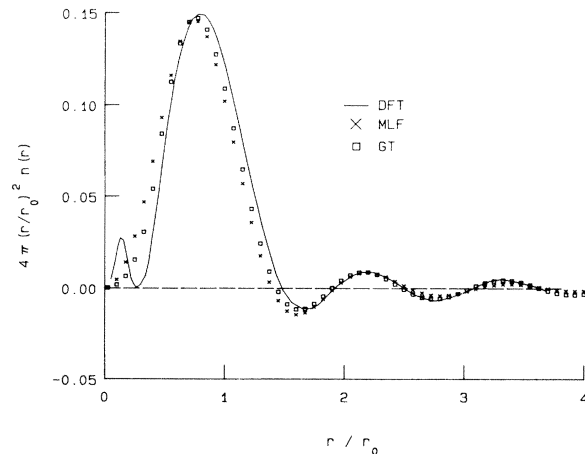


FIG. 9. Electron-charge densities calculated from Eq. (2.11) using the pseudopotentials corresponding to lines 7 and 12 of Table II, at their respective r_s^* , compared with the DFT results of Dagens at $r_s = 2.069$.

about 0.2826, compared with the Vosko-Wilk-Nusair value of 0.27 at the unrenormalized value of $r_s = 2.164$ (however, note that the VS local field gives a slightly higher $k \rightarrow 0$ limit of about 0.286). The enhancement of the $k \rightarrow 0$ limit found by the self-consistent determination of $G(k, r_s^*)$ is probably a reflection of the fact that the conduction-electron compressibility has to conform to the *mixture* compressibility.³² The peak near $2k_F$ found in $[G(k, \lambda^*)]_{\text{MLF}}$ is more pronounced than in the other local fields. The presence of this peak probably gives the MLF dielectric function a Thomas-Fermi-type pole structure even for $r_s^* = 2.767$.

The effective electron-sphere radius r_s^* is usually interpreted in terms of an effective mass of the electrons. This assumes the existence of a k -dependent dispersion relation for the energy, within an effective one-particle Schrödinger equation or one-particle Green function,³³ for the electrons in the liquid metal. However, within the context of the present method we prefer to consider r_s^* as an optimized electron-gas parameter which compensates to some extent the various shortcomings in the theory of the second-order local pseudopotential, linear-response theory, etc. A detailed analysis of the nature of the local

field for the conduction electrons in a liquid metal will be the subject of a future study.

We may conclude that inversion of $[S(k)]_{\text{expt}}$ data using the HNC equation (corrected for bridge terms which are determined self-consistently via a hard-sphere-packing density parameter η) provides a reliable and potentially very powerful method for extracting effective ion-ion potentials, ion-electron pseudopotentials, and the detailed structure of the electron response in liquid metals.

Instead of starting from $S(k)$ obtained from experiments, there is now the possibility of its calculation from first principles using density-functional theory³⁴ for a system of ions and electrons. Such $S(k)$ can then be used within the present inversion method for a completely novel method³⁵ of determining effective pair-potentials which transcend the normal route based on second-order perturbation theory and linear-response theory.

ACKNOWLEDGMENT

We wish to acknowledge the invaluable assistance of Roger Taylor (National Research Council) at every stage of this work, and in making available to us the DRT potentials as well as the MD data on aluminum.

¹M. D. Johnson and N. H. March, Phys. Lett. **3**, 313 (1963).

²T. Gaskell, Proc. Phys. Soc. London **89**, 231 (1966).

³P. Ascarelli, Phys. Rev. **143**, 36 (1966).

⁴Y. Waseda and K. Suzuki, Phys. Status Solidi B **49**, 643 (1972).

⁵W. S. Howells and J. E. Enderby, J. Phys. C **5**, 1277 (1972).

⁶L. E. Ballentine and J. C. Jones, Can. J. Phys. **51**, 1831 (1973).

⁷R. Kumaravadev and D. A. Greenwood, J. Phys. F **4**, 1839 (1974).

⁸Y. Waseda, *The Structure of Noncrystalline Materials* (McGraw-Hill, New York, 1980).

⁹S. K. Mitra, in *Third International Conference on Liquid Metals, Bristol, 1976*, edited by R. Evans and D. A. Greenwood (IOP, Bristol, 1977), p. 147; also S. K. Mitra, P. Hutchinson and P. Schofield, Philos. Mag. **34**, 1087 (1976).

¹⁰R. V. Gopala Rao and R. N. Joarder, Phys. Lett. **67A**, 71 (1978).

¹¹R. Taylor and R. O. Watts, Solid State Commun. **38**, 965 (1981).

¹²K.-C. Ng, J. Chem. Phys. **61**, 2680 (1974).

¹³Y. Rosenfeld and N. W. Ashcroft, Phys. Rev. A **20**, 1208 (1979).

¹⁴N. W. Ashcroft and J. Lekner, Phys. Rev. **145**, 83 (1966).

¹⁵N. W. Ashcroft and D. Stroud, in *Solid State Physics*, edited by H. Ehrenreich, F. Seitz, and D. Turnbull (Academic, New York, 1978), Vol. 33, p. 1.

¹⁶M. Manninen, P. Jena, R. M. Nieminen, and J. K. Lee, Phys. Rev. B **24**, 7057 (1981).

¹⁷L. Dagens, M. Rasolt, and R. Taylor, Phys. Rev. B **18**, 3782 (1978).

¹⁸G. Jacucci, R. Taylor, S. Tenenbaum, and N. Van Doan, J. Phys. F **11**, 793 (1981); MD studies using the DRT potentials

have been reported also by R. D. Mountain, in *Third International Conference on Liquid Metals, Bristol, 1976*, edited by R. Evans and D. A. Greenwood (IOP, Bristol, 1977), p. 62.

¹⁹L. Hedin and B. I. Lundqvist, J. Phys. C **4**, 2064 (1971).

²⁰R. Taylor, J. Phys. F **8**, 1699 (1978).

²¹D. J. W. Geldart and R. Taylor, Can. J. Phys. **48**, 167 (1970).

²²P. Vashista and K. S. Singwi, Phys. Rev. B **6**, 875 (1972).

²³S. Ichimaru and K. Utsumi, Phys. Rev. B **24**, 7385 (1981).

²⁴S. H. Vosko, L. Wilk, and M. Nusair, Can. J. Phys. **58**, 1200 (1980).

²⁵C. R. Leavens, A. H. MacDonald, R. Taylor, A. Ferraz, and N. H. March, Phys. Chem. Liq. **11**, 115 (1981).

²⁶See Ref. 57 contained in Ref. 13; also L. Verlet, Phys. Rev. **165**, 201 (1968).

²⁷G. Jacucci and R. Taylor, J. Phys. F **11**, 787 (1981).

²⁸Al data due to L. Dagens were obtained by courtesy of R. Taylor.

²⁹Y. Waseda, Z. Naturforsch. (in press).

³⁰R. Benedek, Phys. Rev. B **15**, 2902 (1977).

³¹K. K. Mon, N. W. Ashcroft, and G. V. Chester, Phys. Rev. B **19**, 5103 (1979).

³²M. Watabe and M. Hasegawa, in *Properties of Liquid Metals, Proceedings of the Second International Conference of Properties on Liquid Metals*, edited by S. Takeuchi (Taylor and Francis, London, 1973), p. 133.

³³A. H. MacDonald, M. W. C. Dharma-wardana, and D. J. W. Geldart, J. Phys. F **10**, 1719 (1980).

³⁴M. W. C. Dharma-wardana and F. Perrot, Phys. Rev. A **26**, 2096 (1982).

³⁵M. W. C. Dharma-wardana, F. Perrot, and G. Aers, Phys. Rev. A **28**, 344 (1983).